Journal of Modern Optics
Vol. 52, No. 8, 20 May 2005, 1105–1122

Taylor & Francis
Taylor & Francis Group

Fluorescence in the presence of metallic hole arrays

S. H. GARRETT*, L. H. SMITH and W. L. BARNES
Thin Film Photonics Group, School of Physics, University of Exeter, Exeter, EX4 4QL, UK

(*Received 3 September 2004*)

We show that the transmission of light through metallic hole arrays supported by a glass substrate can be tuned by depositing a controlled number of Langmuir–Blodgett layers on top of the hole array. Enhanced transmission is achieved when the number of overlayers is such that the surface plasmon-polariton modes on the two sides of the metal hole array have matched wavevectors. Dye molecules introduced into some of these overlayers allow us to explore the relationship between molecular fluorescence and the transmission properties of the structure, through measurement of the fluorescence lifetime of the molecules. We find there to be little change in the fluorescence lifetime between enhanced and non-enhanced transmission regimes and offer an explanation of our findings in terms of changes in the photonic mode density.

1. Introduction

The demonstration of the enhanced transmission of light through metallic films perforated by an array of sub-wavelength holes has generated considerable interest [1], both in order to understand the underlying physics of the phenomenon and because of the potential it shows for the use of metallic structures in controlling light on sub-wavelength length scales [2]. So far, enhanced transmission has been studied for incident light in the form of plane waves [3]. However, there has been speculation as to whether hole arrays might be usefully employed in the generation of light [4, 5]. In this report we explore how light arising from molecular fluorescence interacts with metallic hole arrays.

It is well established that excited molecules close to metallic surfaces can de-excite via transfer of their energy to surface plasmon-polariton (SPP) modes associated with the metal surface and that such quenching can be significant [6]. The question we wished to address here was whether excited molecules placed over a hole array might couple to the SPP modes supported by such a system, and whether this might significantly alter the fluorescence process, yielding a new way to control the emission of light. In contrast to recent studies of enhanced transmission involving plane waves, the coupling of fluorescence to SPP modes proceeds via high-wavevector near-field components of the oscillating dipole field associated with

*Corresponding author. Email: S.H.Garrett@exeter.ac.uk

Journal of Modern Optics
ISSN 0950–0340 print/ISSN 1362–3044 online © 2005 Taylor & Francis Group Ltd
http://www.tandf.co.uk/journals
DOI: 10.1080/09500340512331323457

individual emitters such as excited molecules, excitons etc. [7]. Before discussing how a hole array might alter such near-field coupling we need to be clear about the process with which one may naturally compare it, namely enhanced transmission of incident plane wave light through metallic hole arrays.

The mechanism by which enhanced transmission is achieved has been the focus of considerable debate but it is now clear that it is a multiple diffraction process enhanced by the involvement of SPP modes [8]. Here we outline our understanding of the mechanism behind the enhanced transmission process as it has an important bearing on the discussion of the results we present in this report.

A cylindrical hole in an optically thick metal film that has a diameter of less than half the wavelength of the light incident upon it does not support any propagating modes; consequently energy can only propagate through such a hole by means of an evanescent tunnelling process. Light that is to be transmitted through such a structure thus needs therefore to be evanescent in character, more specifically the component of the wavevector of the light in the direction through the hole array must be predominantly imaginary. Light incident as a plane wave on a periodic array of such holes generally has a real value of this wavevector component. However, the periodic nature of the array gives rise to diffraction of the incident plane wave, thus providing the possibility for the light to acquire the necessary imaginary part of this wavevector component. Although this diffraction process leads to the possibility of transmission, such transmission is likely to be weak. Furthermore, it makes no use of the metallic nature of the hole array; it is independent of the material from which the hole array is fabricated. This weak transmission may however be enhanced by coupling between light and SPP modes in three distinct ways.

(a) *Process 1*. The incident light may, under appropriate matching conditions discussed below, couple to an SPP mode supported by the surface of the metal facing the incident radiation. SPP modes have the imaginary wavevector required in the direction of propagation through the hole for transmission. Importantly, the enhanced electric field associated with the SPP mode increases the probability of transmission of energy through the holes of the array. On the exit side of the array the attenuated electric field associated with the SPP is scattered by the periodic structure to couple to radiation and the light propagates away from the structure on the exit side of the array.
(b) *Process 2*. Matching conditions may not allow coupling of incident light to SPP modes on the incident side of the metallic hole array, but may be appropriate for coupling the light that is directly, but weakly, transmitted through the array to SPP modes on the exit side of the structure. Again, the enhanced electric field associated with the SPP mode on the exit side increases the probability of transmission of energy through the hole array.
(c) *Process 3*. Matching conditions may be such that both the above processes may occur, for example if the refractive indices of the media bounding each side of the metal film are the same [3]. It is interesting to consider whether, if coupling with SPP modes on both surfaces of the perforated metal film occurs, there is a resonant tunnelling process in which the evanescent fields associated with the SPP modes on the two surfaces interact to further boost the transmission. This question will be addressed later in this report. This has

already been explored for the case of plane wave radiation, and it has been shown with both experimental data and theoretical calculations that under appropriate conditions one can expect a ~10 times increase in transmission when the wavevectors of SPP modes on either side of the metal are brought into resonance [3].

In this work we have set out to discover whether coupled SPP modes affect fluorescence which occurs in close proximity to one of the surfaces of the metallic hole array. It has become clear from recent work that coupled SPP modes can affect the transmission properties of a sub-wavelength hole array in a metal film [1–3], but the effect of such a periodic array on light emitted from such close proximity to the array is not fully understood. One might expect the different decay channels that are available to the emissive molecules in such close proximity to the hole array to affect the emissive decay rate of the molecules. Of course, the way in which the decay channels modify the emissive decay rate depends on whether the decay channels that have been made available are radiative or not. It is helpful at this point to consider the dispersion diagram for the SPP modes supported by a metallic array of sub-wavelength holes.

Our hole array structures comprise a silver film, typically between 50 and 500 nm thick, supported on a fused silica substrate. Consider first such a metal film with no hole array; it supports two distinct SPP modes, one on each surface. The dispersion of these modes (relationship between angular frequency, ω, and in-plane wavevector, $k_{\|}$, the plane being that of the metal film surface) are shown schematically in figure 1 (*a*). There are two distinct modes (solid lines) due to the different refractive indices of the dielectric media. The lower mode corresponds to the SPP mode associated with the metal–substrate interface, since the substrate has the higher refractive index of the two dielectric media. The SPP modes of the two surfaces always have a higher in-plane wavevector than photons propagating in the same direction in the surrounding media (represented by the corresponding air or substrate light lines, dashed lines in figure 1), reflecting the bound nature of these surface modes. Consequently, the modes of such structures cannot be coupled to by free radiation; this coupling can be achieved by the introduction of the hole array into the metal film.

We start by considering one of the more important consequences of adding an array of holes; the effect of adding periodicity into the plane of the structure. (We will discuss the possibility of the SPP modes on either surface of the film coupling via the holes later.) The periodic array allows diffraction (Bragg scattering) to occur, the effect of which on the dispersion of the SPP modes is shown in figure 1 (*b*). First we note that Bragg scattering now allows incident light to couple to the SPP modes, since the scattered SPP modes now fall within the air and substrate light lines. Secondly, we note that the forward and backward Bragg scattered SPP modes on a particular surface intersect at $k_{\|} = 0$. This leads to the formation of standing waves and SPP stop-bands are associated with these standing waves, which complicate the dispersion diagram still further [9]. The opening up of band gaps associated with these stop-bands has been omitted from figure 1 (*b*) for clarity. For the moment, let us concentrate on how normally incident light will interact with the structure. If such light has angular frequency ω_1 it may couple to the SPP mode on the air–metal interface. The EM field associated with the SPP standing wave is enhanced relative to the incident radiation and is evanescent in the direction of the

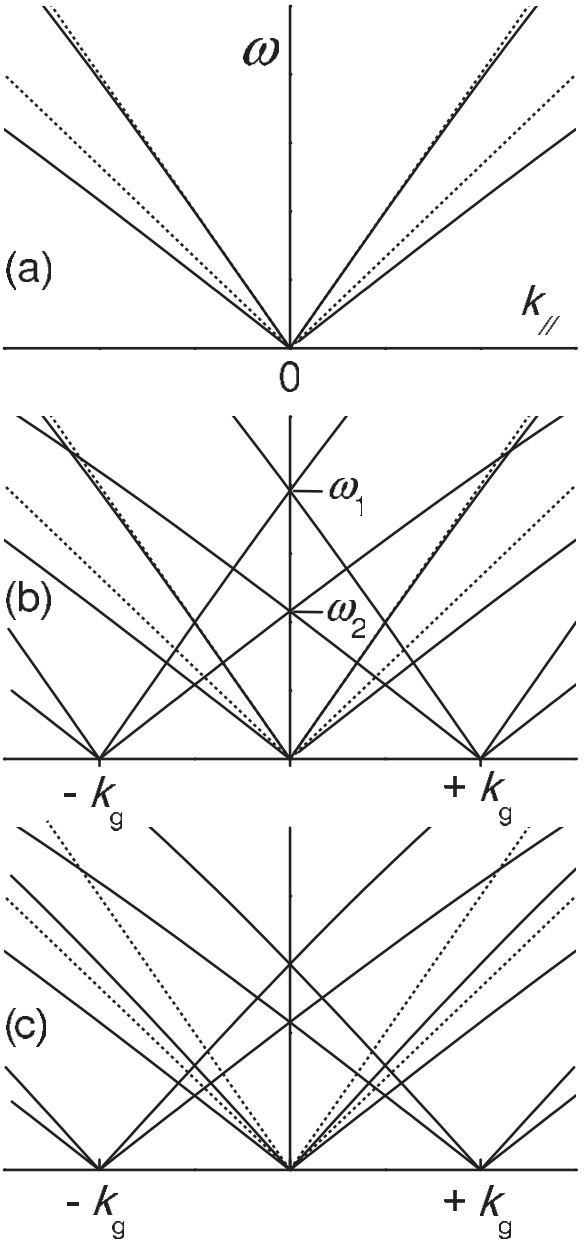

Figure 1. Schematic surface plasmon–polariton dispersion diagrams, i.e. angular frequency (ω) versus in-plane wavevector ($k_{\|}$), for a thick planar metal film bounded on one side by air and on the other by a dielectric. (*a*) The dispersion of SPP modes at metal–air interface and metal–dielectric interfaces. The dashed lines are the associated light lines. (*b*) The effect on the dispersion diagram of adding a periodic modulation to the metal interface; Bragg scattering can now occur, resulting in the original dispersion lines being reproduced at $k_{\|} = \pm 2\pi/\lambda_G$, where λ_G is the period of the modulation. Counter propagating metal–air SPP modes cross $k_{\|}$ at an angular frequency of ω_2, those of the metal–dielectric interface at ω_1. The effect of the surface modulation will produce SPP stop bands, not shown here for clarity. (*c*) The effect on the dispersion of SPP modes of adding a thin dielectric layer onto the metal–air interface; the dispersion lines are pulled down in angular frequency.

plane of the film, and this helps the incident light to traverse the metal, i.e. process 1 as described above. Further, incident light of angular frequency ω_2 that penetrates the holes may couple to the SPP standing wave on the exit side (metal–silica interface) and this again acts as a mechanism to increase the transmission of light, process 2 above.

Now consider the addition of a thin dielectric layer on top of the metal film. The presence of such a layer will increase the in-plane wavevector of the SPP mode on this top metal–dielectric interface; the dispersion diagram for this structure will take the form shown in figure 1 (*c*). The effect of the dielectric layer is to depress the dispersion curve of the SPP mode on the top interface. In this way, as the thickness and/or refractive index of this layer is increased; at some value of the angular frequency the in-plane wavevector of the scattered SPP modes on the top and bottom interfaces will both be equal to zero. When this condition is satisfied, normally incident light may couple via Bragg scattering to both the top SPP and bottom SPP mode, thus providing the means for enhanced transmission, process 3 above. Krishnan *et al*. discussed such matching of SPP modes to achieve enhanced transmission by using a range of index matching oils as one of the bounding media [3]; here we accomplish a similar tuning of this matching condition by varying the thickness of a dielectric overlayer [10].

Before discussing the experiments we undertook to explore the possible effect of these processes on fluorescence that occurred from molecules in close proximity to metallic hole arrays, we should consider what we might expect in view of the preceding discussion. As mentioned earlier, light produced by the process of molecular fluorescence arises from an oscillating dipole moment associated with the transition between the relevant excited molecular level and the corresponding ground state. The near-field of such a dipole source comprises a large number of wavevector components, including many that are evanescent in character. These evanescent near-field components are able to couple directly to high wavevector modes such as SPP modes, provided the fields of such modes overlap the site of the excited molecule, and that such modes exist at the emission frequency of the molecule.

The strength with which coupling between an excited molecule and an SPP mode occurs depends on the strength of the field at the site of the dipole, the emission frequency and the spatial orientation of the oscillating dipole moment. If such coupling is strong enough it may be sufficient to produce a noticeable modification of the fluorescence lifetime of the molecule by providing an additional decay route [7]. Monitoring the fluorescence lifetime in different sample geometries thus affords an excellent method to probe the interaction between molecules and SPP modes, provided one has a good knowledge of the SPP modes of the particular structure in question. We can anticipate two possible ways in which the presence of an array of holes in the metal may lead to changes in the fluorescence lifetime.

First, we know from previous experiments concerning fluorescence above metallic gratings that some modest changes in fluorescence lifetime may be expected over periodically modulated metallic surfaces [11]. These changes were attributed to the fact that the fields reflected by the grating surface were different to those that are produced by reflection from the planar surface. One way to understand how the presence of a surface can change the fluorescence lifetime of a nearby molecule is to consider the field reflected by the surface as a driving field for the emission process; if the reflected field is in phase with the source then the emission will be enhanced and

the fluorescence lifetime reduced, and if the reflected driving field is out of phase with the source then the emission will be inhibited and the fluorescence lifetime increased—clearly the amplitude of the reflected field will dictate the strength of such modifications. The effect of the corrugation is to allow not just a specular reflection, but also diffracted reflected fields. In general, interference between the different reflection processes will not be constructive so that the effect of the specular reflected field is likely to be washed out to some extent [11].

Secondly, it is widely expected that the presence of SPP band edges should make a noticeable modification to the fluorescence lifetime. When the dispersion of any mode is very low, such as at the band edge, the density of states associated with it is high and the fluorescence decay rate will be increased [12], whilst if it lies between the band edges, i.e. in the stop band, the rate will be reduced. It was to test these expectations that we carried out the experiments reported in this paper.

In section 2 we outline the details of our experimental techniques and the fabrication procedures we employed to obtain metallic hole arrays with a variety of well controlled thickness dielectric overlayers. In section 3 we explore how increasing the thickness of a dielectric overlayer changes the transmission of incident plane-wave light, showing that such a technique can be used to produce enhanced transmission. In section 4 we outline our procedure for making fluorescence lifetime measurements and report the results of such measurements on a number of different structures. In section 4 we also provide a summary of our findings together with some suggestions for future work.

2. Fabrication

Figure 2 shows a schematic of the samples used in this study. Silver films were deposited on 25 mm square, 1 mm thick fused silica glass slides by thermal evaporation under vacuum (less than 10^{-6} mbar) at a deposition rate of $0.5\,\mathrm{nm\,s^{-1}}$. A regular square array of 200 ($\pm$5) nm diameter holes with period 415 ($\pm$5) nm were drilled through the metal films using focused ion beam etching (FEI DB 235). The silver film thickness was determined for each sample using calibrated scanning electron microscopy (SEM) images of trenches milled through the silver film using the FIB milling technique.

On each silver-coated slide 16 identical arrays were formed so as to allow a different thickness of overlayer to be deposited on each array. Each array comprised 9 smaller arrays, each of 50 by 50 holes, to form a larger area. Dielectric layers were formed using the Langmuir–Blodgett (LB) technique from 22-tricosenoic, spread from a chloroform solution ($1\,\mathrm{mg\,ml^{-1}}$) onto a subphase of ultra-pure water, indicated by a monitored conductivity of $18\,\mathrm{M\Omega\,cm}$. This optically inert material has an effective isotropic refractive index of $\sim$1.57 at 700 nm. Before the silver surface of each sample was coated with LB layers it was rendered hydrophobic so as to ensure good Y-type deposition, accomplished by exposing the silvered substrate overnight to the vapour from several drops of HMDS (1,1,1,3,3, 3-hexamethyldisilazane) [11].

Using the LB technique, layers of 2, 4, 6 etc. monolayers could be deposited, each having a thickness of $\sim$2.75 nm, thus providing an effective means to adjust the thickness of the dielectric overlayer in a controlled manner. In particular, this allowed us to increase the number of LB layers in order to sweep the dispersion of the

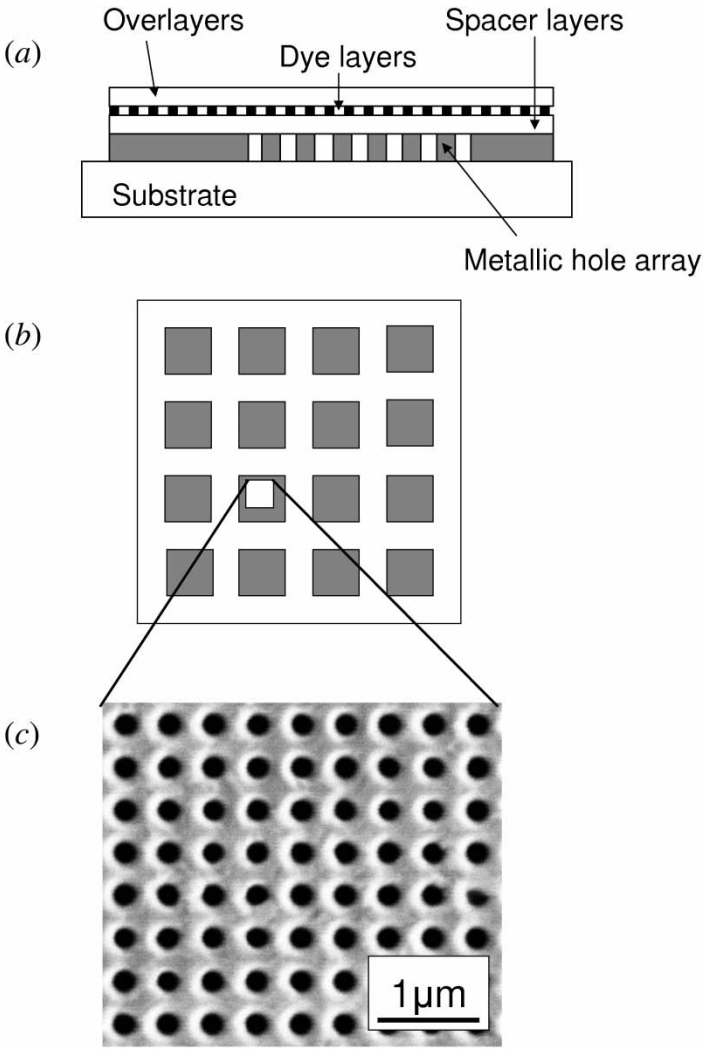

Figure 2. (*a*) Schematic showing a cross-section through the samples used. (*b*) The arrangement of the hole arrays on the substrate. (*c*) A scanning electron micrograph of part of one of the individual arrays.

top SPP mode through that of the lower SPP mode. LB layers were deposited at a surface pressure of $30\,\mathrm{mN\,m^{-1}}$ and transfer ratios of 1.0 ± 0.1 were observed, indicating successful transfer of the layers to the substrate. Particular care was taken to ensure good deposition of the first bilayer of any given LB multilayer by using a low speed of monolayer transfer to the substrate, typically $0.15\,\mathrm{mm\,s^{-1}}$ on the downstroke and $0.10\,\mathrm{mm\,s^{-1}}$ on the upstroke. The combination of slow deposition speeds and the hydrophobic treatment of the surface ensured that no wetting of the silver occurred. Once the first bilayer had been transferred successfully, the dipping speed was increased to $0.30\,\mathrm{mm\,s^{-1}}$ for the downstrokes, $0.25\,\mathrm{mm\,s^{-1}}$ for the upstrokes. The surface pressure was maintained at $30\,\mathrm{mN\,m^{-1}}$ for all depositions.

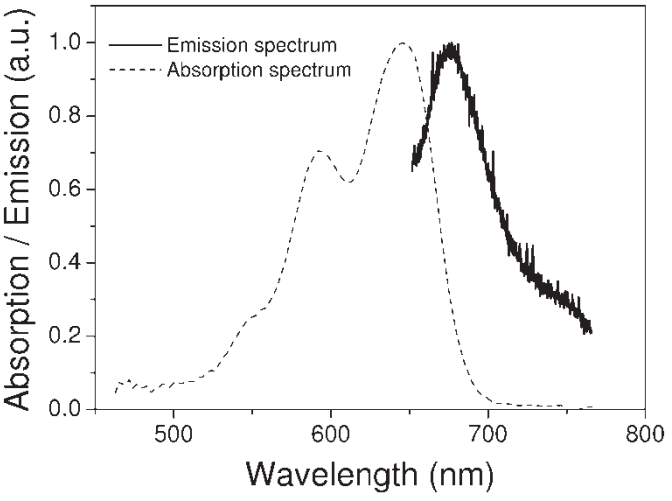

Figure 3. The absorption (dashed line) and emission (solid line) spectra of rhodamine 700. The absorption maximum is around 650 nm and the emission maximum around 680 nm.

To probe the effect of the arrays on molecular fluorescence, we doped the LB material used to form the fifth to eighth LB layers with rhodamine 700 (R700) dye molecules at a doping concentration of R700 : 22-tricosenoic acid molecules of 1:10 000. This low concentration ensured that the measured fluorescence did not exhibit concentration quenching. The emission and fluorescence spectra of the R700 material used are shown in figure 3. Transmission spectra were recorded for normally incident light ($\pm 1^{\circ}$) using an inverted microscope, spectrometer and imaging CCD (charge-coupled device) combination together with a nitrogen-cooled photomultiplier, providing a spectral resolution of 1 nm. Transmission spectra were normalized by reference to the transmission of an uncoated silica glass substrate.

Fluorescence lifetime measurements were made using a time-correlated single-photon counting system (Jobin Yvon IBH Ltd, UK) employing a 635 nm pulsed diode as the pump source (pulse width nominally 50 ps, repetition rate 1 MHz, average power 1 mW focused to a $\sim$500 μm diameter spot). Care was taken to minimize stray pump light through the use of shielding and the use of long pass filters with a transmission of $\sim$80% at wavelengths above 648 nm and blocking $>$99% at 635 nm. Typical lifetimes are shown in figure 4 for two samples. The two decays correspond to fluorescence lifetime data collected from samples consisting of 100 nm silver films on silica substrates with 42 LB layers deposited onto the silver (layers 7–10 are dye doped). One of the decays corresponds to a planar silver region, the other to an array region. For each set of data a theoretical fit to the data is also shown, based on a single exponential decay function of the form $I(t) = I_B + I_0 \exp(-t/\tau)$. To avoid problems due to residual stray pump light, data were only fit in the 8.5 to 25.0 ns time interval—further details of this procedure are given elsewhere [13].

Having outlined the fabrication and characterization techniques, it is convenient to start our discussion of the results we obtained by looking at how increasing the number of LB layers altered the transmission characteristics of the arrays.

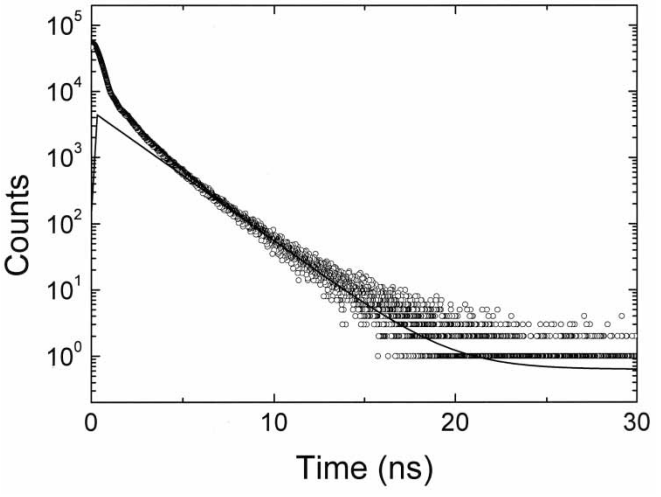

Figure 4. A typical example of time-resolved fluorescence data. The decay consists of data taken from a single sample, consisting of 100 nm silver on a silica substrate, with 42 LB layers deposited onto the silver; layers 7 to 10 are dye-doped layers. The data set is a fluorescence lifetime measurement for light transmitted through the hole array (circles) and the line is the theoretical fit used to obtain the fluorescence lifetime from these data. The data have been fit in the time interval 8.5 to 25 ns with an exponential function of the form $I(t) = I_B + I_0 \exp(-t/\tau)$; the fluorescence lifetime obtained from this fit is 2.20 ± 0.05 ns.

3. Results

The results we obtained are perhaps most easily discussed by dividing them into two parts, differentiated by the thickness of the metal films into which the hole arrays were milled. In section 3.1 we report our results from silver films of 270 ± 5 nm thickness. Following a discussion of these results we then present our results for thinner silver films of 100 ± 5 nm thickness in section 3.2.

3.1 *Results for thick silver films*

3.1.1 Thick silver film—transmission spectra. The transmission spectra for normally incident light as a function of overlayer thickness are shown in figure 5. Looking first at the spectrum in the absence of a dielectric layer, i.e. 0 LB layers, the primary features to note are the peaks at ~510 nm and at ~670 nm. By recalling the dispersion diagram shown in figure 1 (*b*) and noting that the present situation is somewhat more complex because we have a 2-dimensionally periodic structure [2], we can identify these peaks. The peak at ~510 nm arises from the silver–air SPP mode scattered by the Bragg vector of just one of the periodic components, we label this the (1,0) air SPP. We identify the shoulder at ~560 nm as arising from the silver–silica SPP mode scattered by Bragg vectors arising from both periodicities, labelled as (1,1) silica SPP. The peak at ~670 is due to the (1,0) silica SPP.

Again, recalling our introductory discussion, we are interested in how the transmission mediated by the SPP mode on the silica side is affected by adding dielectric layers to the air side of the structure. This is most clearly seen by monitoring the transmission peak associated with the (1,0) scattered silica SPP

mode. As the thickness of the dielectric layer is increased by adding LB layers the transmission associated with this peak rises from ~1.5% for 0 LB layers to a maximum of ~7.4% for a total of 34 LB layers and then falls with the addition of further LB layers. We also note the appearance of a wing on the long wavelength side of the transmission peak. This wing is perhaps due to the measured transmission being a convolution of coupling into the top SPP mode and coupling out of the lower SPP mode, and as the top SPP mode (at $k_{\|}$) moves to lower energy (i.e. longer wavelength), it also broadens. This may only be a partial explanation; there may also be a limited amount of coupling between the top and lower SPP modes. However, we will investigate this possibility further for the case of thin silver films in section 3.2, for which such an effect should be more pronounced. For the moment, we will concentrate on the transmission enhancement observed in thick silver hole arrays.

The data presented in figure 5 show the expected enhancement in transmission as the number of LB layers is increased so as to match the wavevector of the top (silver–LB or air) SPP mode with that of the lower (silver–silica) SPP mode. We can gain further support for this assertion by calculating the effect of the increasing number of LB layers on the dispersion of the top SPP mode. Such a calculation is done by using a plane-wave representation to model an oscillating dipole so as to compute the power lost by such an emitter (representing the fluorescing molecule) as a function of the in-plane wavevector (upon which the plane-wave expansion is based). Peaks in such a power dissipation spectrum correspond to modes, such as SPP modes, into which the energy of the molecule may couple. The details of performing such calculations can be found elsewhere [7]. For the purposes of illustration we calculate the power dissipation spectrum of a source representing an R700 molecule located in air, 20 nm from a semi-infinitely thick silver film; we can deduce the wavevector of the

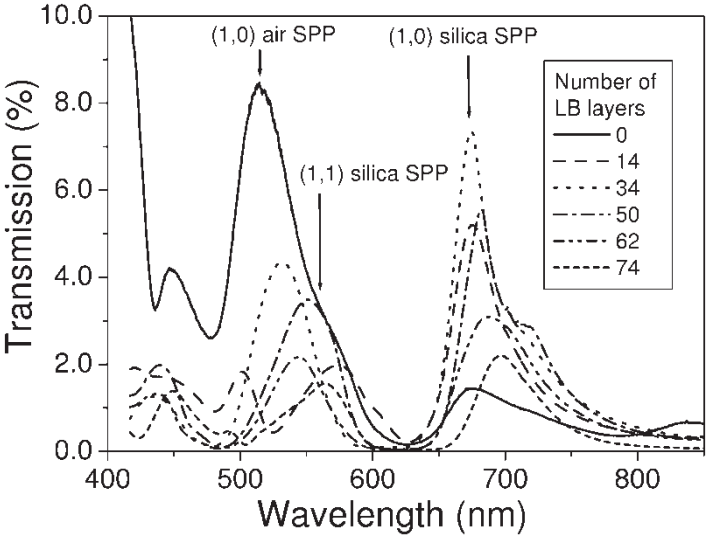

Figure 5. Transmission spectra for 270 nm silver sample for a range of LB overlayer thicknesses from 0 to 74 overlayers. Peaks in the transmission spectra have been identified as being associated with different SPP modes and these peaks are appropriately labelled.

SPP mode associated with the silver–air interface, as shown in figure 6 (*a*). The peak at an in-plane wavevector of $k_{\parallel} \sim 1.05k_0$ (k_0 is the free space wavevector) corresponds to the SPP mode at the silver–air interface, close to the value one obtains by applying the simple formula below [14]:

$$k_{\mathrm{SPP}} = k_0\left(\frac{\varepsilon_1\varepsilon_2}{\varepsilon_1 + \varepsilon_2}\right)^{1/2},$$

where ε_1 and ε_2 are the real parts of the permittivities of the silver and air respectively, using the approximations that $\varepsilon_1 = -19 + 1.2\mathrm{i}$ and $\varepsilon_2 = 1.0$. In figure 6 (*c*) we show a similar calculation, this time for an R700 molecule located 20 nm from the interface between silica ($\varepsilon_2 = 2.13$) and semi-infinite silver.

Between these two power dissipation spectra (figures 6 (*a*) and (*c*)) we plot the power dissipation spectrum for a silver–air interface onto which is introduced an increasing thickness of dielectric corresponding to the LB film material 22-tricosenoic acid used in this study, figure 6 (*b*). These data are plotted as a grey-scale map, light regions indicating high levels of power dissipation and thus mapping out the dispersion of the SPP mode as the thickness of the LB material is increased. We can see that at the wavelength for which this calculation is performed, 670 nm, the silver–LB or air SPP mode has the same wavevector as the silver–silica SPP mode for a LB thickness of ~120 nm, which would correspond to ~44 LB layers. This is in fair agreement with the maximum transmission of ~7% found from the transmission spectra for 34 LB layers (figure 5), given that the calculation ignores the modulated nature of the sample. Note, in these calculations the orientation of the dipole moment was taken to be in the plane of the layers [13].

3.1.2 Thick silver film—fluorescence lifetimes. We recorded fluorescence lifetimes as described above for a range of LB thickness from 14 to 74 layers. In each case the six layers adjacent to the silver were fabricated from pure 22-tricosenoic acid, the next four layers were formed from 22-tricosenoic acid doped with R700. The remaining LB layers were again pure 22-tricosenoic acid. For each thickness we recorded the fluorescence lifetime of the dye over the hole array by pumping the LB covered side of the structure and collecting the fluorescence that emerged through the hole array. As a control we undertook measurements that were otherwise identical, but from a sample that contained no R700 molecules, these layers being replaced by pure 22-tricosenoic acid. Further, we recorded the fluorescence lifetime of the dye over a planar region of the same sample adjacent to the hole array. In this case both pumping and collection of fluorescence took place on the air–LB interface side of the sample, i.e. not through the silica substrate. Again, as a control we also performed the same measurements on a sample that was identical except for being undoped with R700. We next explore whether there is any discernable change in fluorescence lifetime as the LB film thickness sweeps through the condition for matching the SPP modes on the top and bottom surfaces of the metal. This condition is expected to be met with a LB film thickness of ~44 layers (i.e. ~120 nm). The fitted fluorescence lifetime data, plotted as a function of LB film thickness, are shown for both planar and hole array sample structures in figure 7. It is clear from these data that there is no significant modification of the fluorescence lifetime as the LB film thickness is swept through that of the expected matching condition, although

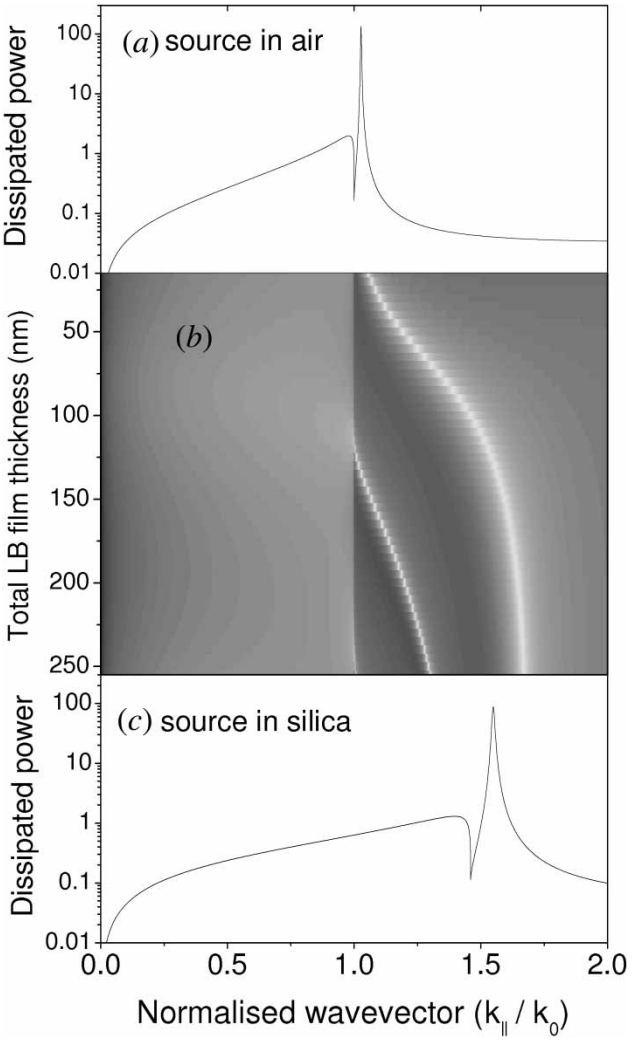

Figure 6. Calculated power dissipation spectra: (*a*) the power dissipation spectrum for a source embedded in air and located 20 nm from the interface with semi-infinite silver. (*c*) The result of a similar calculation where silica glass replaces the air. (*b*) The power dissipation spectrum is plotted as a grey scale to show how the silver–air SPP mode disperses as the thickness of dielectric LB layers deposited onto the silver–air interface is increased. The calculations are based on the dye molecules' dipole moments lying in the plane of the LB film. White regions correspond to high levels of power dissipation. Note that for LB thicknesses above ~120 nm a waveguide mode is also supported.

there is a consistent difference found between the fluorescence lifetimes for the molecules over the hole array and the molecules over the planar regions.

3.1.3 Thick silver film results—discussion. Let us first consider the fluorescence lifetimes we have measured for the molecules over the planar Ag regions. It is relatively straightforward to calculate how the fluorescence lifetime should vary as a function of overlayer thickness using the power dissipation approach

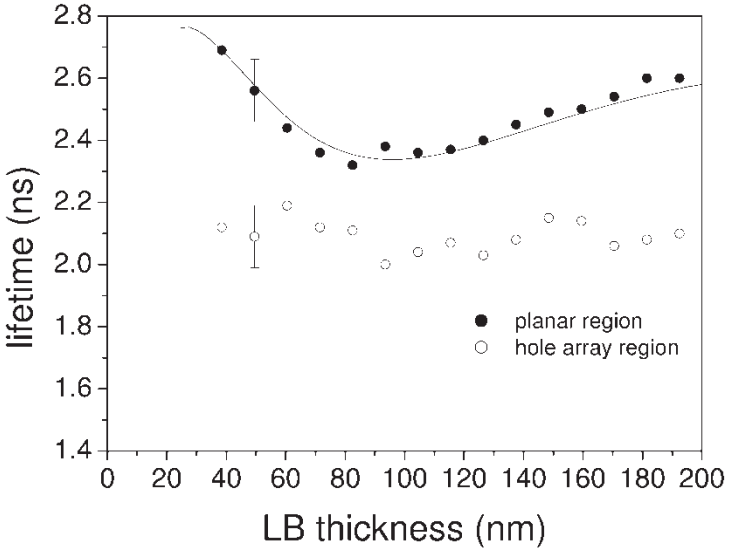

Figure 7. The measured fluorescence lifetimes (as determined by fitting to the experimental data) as a function of LB layer thickness for dye molecules over planar 270 (±5) nm thick silver and over the same thickness of silver perforated with a periodic square array of 200 (±5) nm with a period of 415 (±5) nm. Also shown is the calculated dependence of the fluorescence lifetime for the planar region experimental data set. The calculations are based on quantum efficiency $q = 0.4$ and a horizontal dipole moment orientation. To simplify the calculations, emission has been taken as a single wavelength, 670 nm. Also included are sample error bars.

discussed above [7]. If we integrate the power dissipated over all in-plane wavevectors so as to obtain the total power lost then we have a direct measure of the lifetime, since the total power lost is directly related to the decay rate of the emitter, which in turn is the reciprocal of the fluorescence lifetime. The results of such a calculation are shown as the solid line accompanying the experimental data points for the planar region in figure 7. The calculation takes into account the orientation of the dipole moment associated with the dye molecules (in the plane of the film).

The good agreement between such a calculation and the experimental data gives us confidence that we understand the nature of the changes induced in the fluorescence lifetime as the overlayer thickness is increased in this case. The data from the hole array regions show very little dependence on overlayer thickness and are typically only ~85% of the value for the corresponding planar regions. To understand this reduction in fluorescence lifetime it is instructive to look at the effect the planar silver film has on the lifetime of the dye molecules. We used the same model with which we produced the theoretical data in figure 7 to calculate that the presence of a silver interface ~25 nm from the dye molecules increases their lifetime by ~8% over the lifetime that they would have if the silver film was removed and replaced with LB material. This increase in lifetime arises because the specular reflection of the planar silver film acts to drive the emitter out of phase, thereby reducing the probability of emission. The introduction of holes will disrupt this reflected field in a similar manner to the corrugated surface investigated in [11, 15],

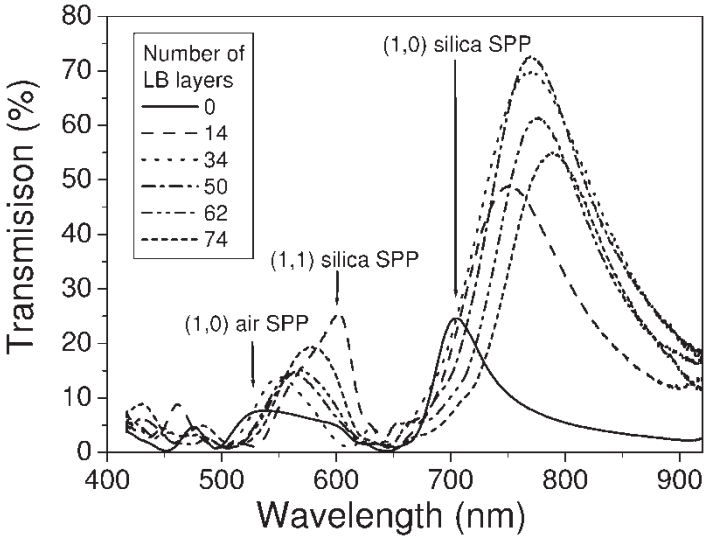

Figure 8. Transmission spectra for 100 nm silver sample for a range of LB overlayer thicknesses from 0 to 74 overlayers. Peaks in the transmission spectra have been identified as being associated with different SPP modes and these peaks are appropriately labelled.

i.e. the presence of diffracted orders will tend to wash out the effect of the specular reflection. Since the presence of the planar silver film acts to increase the lifetime, we now expect that introducing a hole array will reduce the lifetime, in accord with what we find experimentally, although the reduction in lifetime is somewhat greater than we might expect.

Having accounted for the overall trend we now turn our attention to the lack of significant modification of the fluorescence lifetime as the thickness of the overlayer is increased. The change in the fluorescence lifetime is determined by the coupling of the excited fluorophore to the optical modes of the structure. If this coupling is strong then the lifetime will be reduced, if it is weak the lifetime may be extended. We need to consider two aspects; first, does the fluorophore couple to the SPP modes on both the upper and lower interfaces? Second, will such coupling, if it occurs, cause a change in lifetime? For the thick planar silver film considered here (270 nm) one expects the field of the SPP mode on the silica side of the silver to be heavily attenuated by the metal so that it will play no part in the decay of the R700 molecules. Now, although the addition of holes to the silver film clearly affects the transmission of normally incident light, it does not appear to have had any significant effect on the fluorescence lifetime. Before discussing this further let us look at the results from thin silver films.

3.2 *Results for thin silver films*

To test whether a reduced silver thickness would produce coupling between the SPP modes of the two surfaces and whether this in turn might produce significant lifetime modification, we examined a second set of samples identical to the first except for the fact that the silver was 100 ± 5 nm thick.

3.2.1 Thin silver film—transmission measurements. Transmission spectra as a function of overlayer thickness for normally incident light are shown in figure 8. Comparing the transmission of the uncoated (i.e. 0 LB layers) thin silver film with that of the thick silver film in figure 5 shows two striking differences. The first is that the much higher value of the transmittance, ~25% versus ~8%, and the second is the relative strength of the different features. The much higher overall transmission is a direct result of the greatly reduced thickness of the thin silver film compared with the thick silver film. The transmission spectrum of the thin silver film is dominated by the peak associated with (1,0) silica SPP, whilst that for the thick silver film is dominated by the peak associated with the (1,0) air SPP.

As in the case of the thick silver film, we concentrate on the transmission peak associated with (1,0) silver–silica SPP. Again, as for the thick silver film, we find that as the number of LB layers increases the transmittance of this peak also rises from ~25% (at 0 LB layers), reaching a maximum of ~74% at ~50 LB layers (~140 nm). In contrast to the thick silver sample, the position of this peak changes as the LB layer thickness is increased towards the value giving maximum transmission, from ~704 nm at 0 LB layers to ~770 nm at 50 LB layers. One possible explanation for this shift might be an interaction between the SPP modes on the top and bottom surfaces that has possibly become significant as a consequence of the reduction in silver film thickness. This might perhaps also account for the maximum transmission occurring at ~140 nm (50 LB layers) rather than the ~94 nm (34 LB layers) seen for the thick silver film (figure 5) and the ~120 nm (44 LB layers) of the calculation (figure 6).

3.2.2 Thin silver film—fluorescence lifetimes. In previous work fluorescence from Eu^{3+} ions above a thin silver film was studied [16] and evidence was found for the SPP mode on the lower surface having an effect on the measured fluorescence lifetime for a silver film thickness below ~70 nm. We undertook similar measurements using the R700 molecules employed in this study as a control. For a planar 100 nm thick silver film, the evanescent field penetration from the SPP modes on either side of the silver film is negligible, but the presence of an array of holes in the silver might be expected to increase the field penetration through the film and, therefore, lead to possible cross-coupling between the SPP modes associated with each side of the silver film, in turn affecting the photonic mode density at the site of the R700 molecules placed in close proximity to the hole array. The results of such an experiment are shown in figure 9. Here we have plotted the measured lifetimes for the planar regions of a sample with 100 nm silver film. As expected, the data are very similar to the planar region results for the 270 nm sample as plotted in figure 7, since the evanescently decaying SPP fields are effectively blocked by the 100 nm silver film. However, it is clear that the result for the hole array region is rather different; rather than the reduction of fluorescence lifetime to ~85% of the planar value as seen for the thick silver film (figure 7), the reduction here is more modest. Using the results from other work [17] we can estimate that a planar silver film of thickness 25 nm has the same effect as our perforated 100 nm film, at least in terms of field penetration. To explore this further we have also plotted the fluorescence lifetimes measured for a similar sample with a planar 23 nm silver film in figure 9. The effect is quite pronounced; the fluorescence lifetime is now reduced to ~70% of 100 nm (or 270 nm) planar value. Calculations similar to those

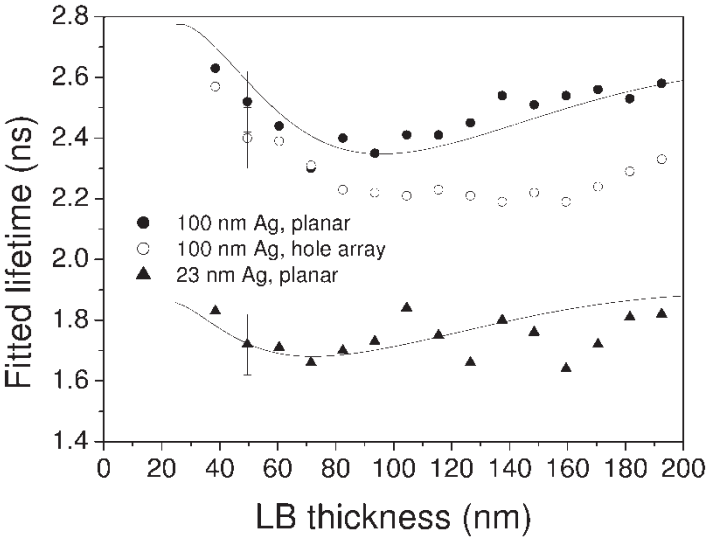

Figure 9. The measured fluorescence lifetimes (as determined by fitting to the experimental data) as a function of LB layer thickness for dye molecules over planar 100 (±5) nm thick silver and over the same thickness of silver perforated with a periodic square array of 200 (±5) nm holes with a period of 415 (±5) nm. Experimentally determined results are also included for the same measurements for dye molecules above a planar 23 nm thick silver film. Also shown is the calculated dependence of the fluorescence lifetime for each of the planar region experimental data sets. The calculations are based on quantum efficiency $q = 0.4$ and a horizontal dipole moment orientation. To simplify the calculations, emission has been taken as a single wavelength, 670 nm. Also included are sample error bars.

performed for figure 7 allowed the theoretical curves for the thin planar silver films to be added to figure 9 as shown. Details of this calculation, notably examination of the power dissipation spectrum (not shown) indicate that the dominant cause of the lifetime modifications is the presence of the SPP mode associated with the silver–silica interface.

4. Discussion

We can summarize our results as follows. We found that the fluorescence lifetimes of molecules over silver films perforated by hole arrays is not radically different from that of the same molecules over planar silver films. This was found to be true for both the thick (270 nm) and thinner (100 nm) silver films studied; indeed, the lifetimes over these two different types of hole array were found to be very similar, in both cases being somewhat shorter than for the equivalent planar silver samples. We have argued that the reduction of fluorescence lifetime for hole array samples compared with planar samples arises from the periodically modulated nature of the silver reducing the effective reflected field that acts to drive the emitting molecules.

These observations remained effectively unchanged even when we adjusted the thickness of the LB layers in order to match the in-plane wavevectors of the SPP modes on either side of the silver film, which in principle allowed the possibility of the modes on either surface to interact. The fact that we observed no change in the fluorescence lifetime in the vicinity of this coupling condition can be ascribed to

a variety of factors, some of which have been discussed earlier. The key inference to make from these observations is that the lack of modification of fluorescence lifetime implies that there is little if any change in the photonic mode density at the site of the emitting molecules. Consider first the contribution to the mode density made by the SPP associated with the silver–LB–air interfaces; as noted above, the effect on the fluorescence lifetime comes from SPP modes propagating in all in-plane directions, and though the in-plane wavevector of these modes is modified by increasing the number of LB layers overlying the dye doped region, the net effect on the mode density, and hence the fluorescence lifetime, appears to be weak since the oscillations seen in figures 7 and 9 are weak. If the wavevector of the SPP modes on the two sides of the silver were matched *and* the fields of the two modes penetrated (evanescently) through the holes sufficiently, one might perhaps have expected an interaction between the two modes and therefore a modification of the fluorescence lifetime. Although we found possible signs of coupling between the SPP modes on the two sides of the silver for the thin silver film in the transmission data, there is no evidence from the fluorescence lifetime data of any influence coming from the silver–silica interface, whether by SPP modes interacting or simply by the field of the silver–silica SPP mode penetrating the silver to the extent of directly adding to the mode density at the site of the R700 molecules.

One might expect the orientation of the dipole moment associated with the R700 molecules, lying in the plane of the structures, to make coupling to the SPP modes weak, rendering our search for such an effect rather difficult. However, our results on very thin planar silver (23 nm) in figure 9 show that if a planar silver film is thin enough we can indeed discern effects on the fluorescence lifetime due to the lower silver interface since the fluorescence lifetime is significantly reduced for R700 molecules above a 23 nm silver film compared with 100 nm silver film. Interestingly there is still no modulation of fluorescence lifetime with increased overlayer thickness even in this case. Of course, we might also consider the exact distribution of dye molecules over the hole array—perhaps there is no coverage over the holes at all? SEM micrographs (not shown) clearly indicate that the LB films *do* successfully bridge the holes. This leads us to another consideration; there is of course a range of molecular sites over the hole array, since the holes are far larger in diameter than the dimensions of the molecules, and these sites will have different mode densities which in turn will lead to different fluorescence lifetimes. Although our technique averages out such effects it is perhaps still reasonable to expect that if significant changes do arise in mode density, even only in specific regions, we might observe some interesting effects, not least because the relative coverage of hole to remaining planar film is $\sim$20%.

What then are we to make of our results? First we should note that one must be cautious about extrapolating ideas developed from considering the response of metallic nanostructures to plane-wave light to the case of emission produced by excited molecules near the metallic structures. Plane waves contain only one in-plane wavevector component, whilst the near-fields produced by molecular scale emitters contain a wide range of wavevectors. Secondly, we have found further evidence that the SPP modes on either side of the metal film do not interact unless the metal film is very thin, and the presence of a hole array does not increase the interaction between the two modes as much as one might perhaps have expected, and therefore only thin perforated films produce evidence of this interaction, films that are thin enough to produce interaction between the SPP modes even in the case of planar (unperforated)

films. Certainly, metal films need to be of order or less than the 100 nm perforated silver film used in this study for the interaction to be observed; this is consistent with the recent findings of Degiron *et al*. [17]. Thirdly, the lack of any radical modification of the fluorescence lifetime over the hole array is a direct indication that the photonic mode density at the site of the molecules is not much changed by the matching of the SPP wavevectors. This is not altogether unexpected; the presence of new or altered modes may not necessarily change the fluorescence lifetime since, as these modes become available, coupling to other modes may become weaker, which is something we have observed before [18]. Although we have not found significant modifications to fluorescence lifetimes, this does not mean that the use of arrays in this context is of no value, as recent results attest to a wealth of other opportunities. Our results may not provide immediate new applications but they have helped to clarify the physics underlying the enhanced transmission of metallic hole arrays and this is an interesting avenue that demands further exploration.

Acknowledgments

The authors would like to thank the EPSRC for partially funding this work. We also thank the European Commission under project FP6 NMP4-CT-2003-505699—Surface Plasmon Photonics. The authors would like to thank E. Deveaux at Laboratoire des Nanostructures, Université Louis Pasteur, France for milling the hole arrays and providing scanning electron micrographs.

References

[1] T.W. Ebbesen, H.J. Lezec, H.F. Ghaemi, *et al*., Nature **391** 667 (1998).
[2] W.L. Barnes, A. Dereux and T.W. Ebbesen, Nature **424** 824 (2003).
[3] A. Krishnan, T. Thio, T.J. Kim, *et al*., Opt. Commun. **200** 1 (2001).
[4] Y. Liu and S. Blair, Opt. Lett. **28** 507 (2003).
[5] Y. Liu and S. Blair, Opt. Express **12** 3686 (2004).
[6] W.H. Weber and C.F. Eagen, Opt. Lett. **4** 236 (1979).
[7] W.L. Barnes, J. Mod. Opt. **45** 661 (1998).
[8] W.L. Barnes, W.A. Murray, J. Dintinger, *et al*., Phys. Rev. Lett. **92** 107401 (2004).
[9] W.L. Barnes, T.W. Preist, S.C. Kitson, *et al*., Phys. Rev. B **54** 6227 (1996).
[10] S. Wedge, S.H. Garrett, I. Sage, *et al*., J. Mod. Opt. (in press) (2004).
[11] P. Andrew and W.L. Barnes, Phys. Rev. B **64** 125405 (2001).
[12] J.P. Dowling, M. Scalora, M.J. Bloemer, *et al*., J. Appl. Phys. **75** 1896 (1994).
[13] S.H. Garrett, J.A.E. Wasey and W.L. Barnes, J. Mod. Opt. **51** 2287 (2004).
[14] H. Raether, *Surface Plasmons* (Springer-Verlag, Berlin, 1988).
[15] R.M. Amos and W.L. Barnes, Phys. Rev. B **59** 7708 (1999).
[16] R. Amos and W.L. Barnes, Phys. Rev. B **55** 7249 (1997).
[17] A. Degiron, H.J. Lezec, W.L. Barnes, *et al*., Appl. Phys. Lett. **81** 4327 (2002).
[18] P.T. Worthing, R.M. Amos and W.L. Barnes, Phys. Rev. A **59** 865 (1999).